Original article

Effect of Radionuclide Activity Concentration on PET-CT Image Uniformity

**Francis Hasford[1,2,3], Bronwin Van Wyk[1], Thulani Mabhengu[1], Mboyo Di Tamba Vangu[1],
Augustine Kwame Kyere[2], John Humphrey Amuasi[2]**

[1]Department of Nuclear Medicine, CM Johannesburg Academic Hospital, University of the Witwatersrand, Johannesburg,
South Africa, [2]Department of Medical Physics, School of Nuclear and Allied Sciences, University of Ghana, [3]Medical Radiation
Physics Centre, Radiological and Medical Sciences Research Institute, Ghana Atomic Energy Commission, Accra, Ghana

Abstract

Assessment of radionuclide activity concentration on positron emission tomography-computedr tomography (PET-CT) image uniformity has been carried out quantitatively. Tomographic PET-CT images of cylindrical phantom containing F-18 fluorodeoxyglucose (FDG) activity concentration was acquired and used for the assessment. Activity concentrations were varied and PET-CT images were acquired at the constant acquisition parameters of time, matrix size, and reconstruction algorithm, respectively. Using midtransaxial image slices, quantitative index of nonuniformity (NU), and coefficient of uniformity variation were estimated for the different activity concentrations. Maximum NUs of 17.6%, 26.3%, 32.7%, 36.2%, and 38.5% were estimated for activity concentrations of 16.87 kBq/mL, 14.06 kBq/mL, 11.25 kBq/mL, 8.43 kBq/mL, and 5.62 kBq/mL, respectively. The coefficient of uniformity variation established an inverse quadratic relationship with activity concentration. Activity concentrations of 16.87 kBq/mL, 14.06 kBq/mL, 11.25 kBq/mL, 8.43 kBq/mL, and 5.62 kBq/mL produced uniformity variations of 1.47%, 2.52%, 4.23%, 5.12%, and 4.98%, respectively. Increasing activity concentration resulted in decreasing coefficient of uniformity and hence, an increase in image uniformity. The uniformity estimates compared well with the standards set internationally.

Keywords: Activity concentration, counts of activity, image uniformity, positron emission tomography-computed tomography, radionuclide

Introduction

The acquisition of accurately coregistered anatomic and functional images is a major strength of the positron emission tomography-computed tomography (PET-CT) integrated system. However, the additional advantage of this approach is the possibility to use the CT images for attenuation correction of the PET emission data, eliminating the need for a separate, lengthy PET transmission scan. The use of the CT scan for attenuation correction not only reduces whole-body scan by 30-40% but also provides essentially noiseless attenuation correction factors (ACFs) compared to those from standard PET transmission measurements.[1-4] Since the attenuation values are energy-dependent, the correction factors derived from a CT scan at mean photon energy of 70 keV must be scaled to the PET energy of 511 keV.[5,6] Integrated PET-CT system has become an established diagnostic modality that is extensively used in the oncology for tumor diagnosis, staging, and radiotherapy treatment planning and monitoring in cardiology for myocardial viability and perfusion, and in neurology for perfusion and neuroreceptor imaging.[7,8]

Most image distortions in PET-CT images can be associated with distortions of the CT images that propagate into the PET images through the use of CT-based attenuation correction. Similarly, pitfalls arise from the limitations of the standard approach to CT-based attenuation correction that does not account for the presence of artificial implants or CT contrast agents.[3] Furthermore, misalignment effects between the CT and

Address for correspondence:
Mr. Francis Hasford, Medical Radiation Physics Centre, Radiological and Medical Sciences Research Institute, Ghana Atomic Energy Commission,
P.O. Box LG 80, Legon, Accra, Ghana. E-mail: haspee@yahoo.co.uk

PET acquisitions may create biases in the reconstructed PET images. An advantage of PET imaging is its ability to accurately quantify the distribution of the injected tracer in the body noninvasively. This accuracy relies on several corrections during the image acquisition and reconstruction process but also depends on the accurate knowledge of the amount of injected activity. One of the most widely used metrics in PET imaging is the standard uptake value (SUV) that is defined as:

$$\text{SUV} = \frac{\text{Activity concentration in a region of interest (kBq / mL)}}{\text{Injected activity (MBq) / patient weight (kg)}} \quad (1)$$

Physicists are recommended to conduct a qualitative and quantitative review of PET-CT image uniformity during acceptance testing and at least once in every quarter.[9,10] Qualitative review includes evaluation of the uniformity and noise characteristics of the images and quantitative review includes evaluation of the accuracy of the SUV calibration and the axial variation of the average SUVs. The National Cancer Institute's (NCI) manual of procedures for PET and PET-CT systems recommends an acceptance criterion of less than 10% for axial variation in PET-CT image uniformity.[8] The International Atomic Energy Agency's Human Health Series (HHS) publication on quality assurance for PET and PET-CT systems (HHS No. 1) also recommends a nonuniformity (NU) estimate of less than 1.05 × reference NU.[9] This study evaluates the effect of activity concentration on the uniformity of PET-CT images.

Materials and Methods

A PET-CT integrated system (Biograph 40, Siemens, Memphis, Tennessee, USA) was used in acquiring images for the study. The system has a 40-slice CT component that provides a 360° full scan of an average patient in approximately 40 s. The PET component uses lutetium oxyorthosilicate (LSO) detector that produces fast scintillation, high light yield, and fast light decay time. Dimensions of the LSO detectors are $4 \times 4 \times 20$ mm^3, giving it a high resolution capability. The system has a 70-cm spacious gantry opening for easy and flexible patient positioning, enhanced patient comfort, and convenience. Cylindrical phantom (Siemens, Memphis, Tennessee, USA) was used for the PET-CT image uniformity assessment. The phantom has internal diameter of 190 mm and a volume of 6.58×10^6 mm^3. The cylinder comes with a lid that has three fill ports through which water or activity is introduced into the phantom.

The cylindrical phantom was filled with water such that it was about three quarters full and 111 MBq F-18 fluorodeoxyglucose (FDG) activity was injected into it. The cylinder was covered with the lid and the phantom

was repeatedly inverted to thoroughly mix the activity with the water. More water was added to the cylinder until it was almost completely full. It was repeatedly inverted again to achieve uniform distribution of activity in the phantom. With the phantom lid still closed, the water was injected gradually through the fill port into the phantom using a syringe until the phantom was completely full. The resultant activity concentration was estimated to be 16.87 kBq/mL. Air bubbles were removed by gently shaking the phantom.

The phantom was mounted to the patient bed such that its long axis was parallel to the axis of the scanner and its positioning was done using lasers, as shown in Figure 1. Scout view of the phantom was first taken with the CT scanner and used to define the scan boundaries of the phantom. The scan length on the PET system was a two-bed position with the phantom centered in the axial extent of the combined two-bed positions. The CT and PET phantom scans were acquired using standard clinical protocols for body PET-CT imaging in accordance with the manufacturer's recommendation. The PET scan was performed at 4 min per bed position.

Axial PET-CT images of the phantom were acquired with the system at 3-mm slice thicknesses. Slices corresponding to the uniform long active part of the phantom were reconstructed with all the corrections applied using the system software. Calculated attenuation correction was applied using the corresponding CT images to avoid noise propagation. Reconstructed transaxial and sagittal slices of the images were displayed and carefully inspected visually for artifacts. One midtransaxial slice was selected for the PET-CT image uniformity assessment by estimating its quantitative index of nonuniformity NU and the coefficient of uniformity variation. The entire study was repeated at reduced F-18 FDG activity concentrations of 14.06 kBq/mL (injection

Figure 1: Cylindrical phantom under scanning

of 92.5 MBq activity), 11.25 kBq/mL (injection of 74 MBq activity), 8.43 kBq/mL (injection of 55.5 MBq activity), and 5.62 kBq/mL (injection of 37 MBq activity) and their corresponding nonuniformity NU indices and coefficients of variation were estimated. The estimated uniformity indices and coefficients of variation for the five activity concentrations were then compared to assess the effect of radionuclide activity concentration on PET-CT image uniformity.

For each activity concentration, one midtransaxial image slice was chosen for uniformity analysis on the PET-CT computer system. Quantitative index of nonuniformity NU and coefficient of variation were estimated by drawing a circular area of 175-mm diameter centered inside the selected image slice. As shown in Figure 2, a total of 177 square regions of interest measuring 10×10 mm^2 were drawn on each slice inside the circular area. For each region of interest (ROI) k in image slice i, the maximum, average, and minimum counts of activity inside the kth ROI were identified and recorded.

The nonuniformities (NUs) in individual ROIs across the image slice were estimated using the NU expression in Equation 2.[10] The maximum NU among the 177 ROIs in each selected image slice was identified. Coefficient of uniformity variation (CV) across the image slice was also estimated using Equation 3.[10]

$$NU_{slice=i} = Max\left\{^{NU_1}_{NU_2}\right\} = Max\left\{\begin{array}{c}\frac{Max(C_k)-Ave(C_k)}{Ave(C_k)}\times100\\\frac{Ave(C_k)-Min(C_k)}{Ave(C_k)}\times100\end{array}\right\} \quad (2)$$

$$CV_{slice=i} = \frac{\text{St Dev of counts of activity in slice}}{\text{Average count of activity}}\times100 \quad (3)$$

$$= \frac{SD_{slice=i}}{Ave(C_k)}\times100$$
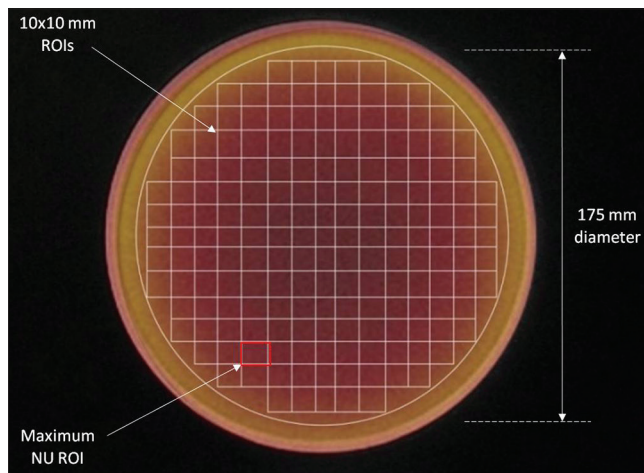
Figure 2: PET-CT image slice of phantom (with 8.43 kBq/mL F-18 FDG)

where, standard deviation

$$(SD)_{slice=i} = \sqrt{\frac{1}{(N_{ROIs}-1)}\sum_{k=1}^{k}\left[C_k - Ave(C_k)\right]^2}\text{ , and}$$

denote the number of the square ROIs inside the 175 mm diameter circle.

Results

Table 1 presents NU estimates in the ROIs for the five activity concentrations and Table 2 presents the coefficients of uniformity variation in the concentrations.

A variation of the estimated image uniformity with activity concentration is graphically presented in Figure 3.

Discussion

NUs in the 177 ROIs for the five activity concentrations are presented in Table 1. The NUs were estimated to assess the PET-CT system's response to homogeneous activity distribution on the micro level. The higher the NU value in a ROI, the less uniform the activity concentration in that particular region. From the study, highest and least NU estimates were attained in image slices having activity concentrations of 5.62 kBq/mL and 16.87 kBq/Ml, respectively. The study observed a pattern where the maximum NU in ROIs increases with decreasing activity concentration. Activity concentrations of 16.87 kBq/mL, 14.06 kBq/mL, 11.25 kBq/mL, 8.43 kBq/mL, and 5.62 kBq/mL produced maximum NUs of 17.6%, 26.3%, 32.7%, 36.2%, and 38.5%, respectively. The NU estimates, however, represent only single image slices and hence, may not be generalized for the entire volume of phantom.

Given that PET imaging for different activity concentrations were all carried out in equal time durations of 4 min per bed position, F-18 FDG with higher activity concentration was seen to accumulate more counts of activity compared with less activity
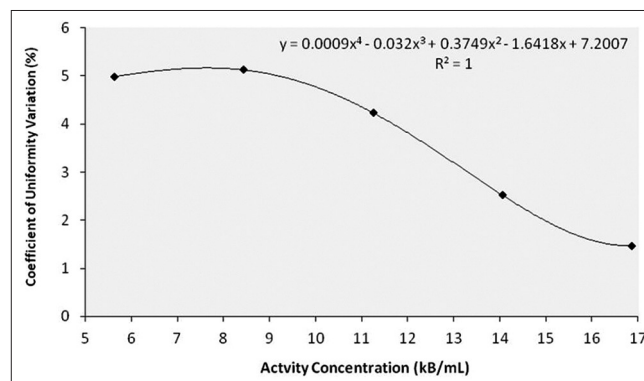
Figure 3: Variation of image uniformity with activity concentration

Table 1: Nonuniformities in ROIs for different activity concentrations

Region of interest	16.87 kBq/mL Counts of activity (C_k)			16.87 kBq/mL Nonuniformity (% NU)		14.06 kBq/mL Counts of activity (C_k)			14.06 kBq/mL Nonuniformity (% NU)		11.25 kBq/mL Counts of activity (C_k)			11.25 kBq/mL Nonuniformity (% NU)		8.43 kBq/mL Counts of activity (C_k)			8.43 kBq/mL Nonuniformity (% NU)		5.62 kBq/mL Counts of activity (C_k)			5.62 kBq/mL Nonuniformity (% NU)	
	Max	Ave	Min	NU_1	NU_2	Max	Ave	Min	NU_1	NU_2	Max	Ave	Min	NU_1	NU_2	Max	Ave	Min	NU_1	NU_2	Max	Ave	Min	NU_1	NU_2
ROI 1	1031	936.4	846	10.6	9.7	492	395.8	334	24.3	15.6	275	233.3	183	17.9	21.6	107	88.2	75	21.3	15.0	78	63.4	55	18.3	13.2
ROI 2	1023	933.3	835	9.6	10.5	495	411.8	353	20.2	14.3	292	256.1	194	14.0	24.2	100	89.3	76	12.0	14.9	73	66.2	52	10.3	21.5
ROI 3	1033	942.3	828	9.6	12.1	482	418.4	354	15.2	15.4	301	244.5	192	23.1	21.5	105	87.7	66	19.8	24.7	69	59.3	49	16.4	17.4
ROI 4	1037	918.4	831	12.9	9.5	468	419.3	363	11.6	13.4	288	232.6	172	23.7	26.1	99	88.4	77	12.0	12.9	78	63.2	52	23.4	17.7
ROI 5	1036	945.7	842	9.5	11.0	495	410.8	323	20.5	21.4	261	223.6	182	16.7	18.6	100	87.6	78	14.1	11.0	75	65.4	59	14.7	9.8
ROI 30	1043	983.6	810	6.0	17.6	498	415.3	316	19.9	23.9	266	215.6	181	23.4	16.0	111	90.7	67	22.4	26.1	67	60.2	52	11.3	13.6
ROI 62	1029	963.5	843	6.8	12.5	502	428.5	353	17.2	17.6	281	236.3	159	18.9	32.7	103	89.2	78	15.5	12.5	78	61.1	52	27.7	14.9
ROI 151	1022	957.3	818	6.8	14.6	503	453.2	377	11.0	16.8	289	236.7	170	22.1	28.2	99	86.7	78	14.2	10.0	81	58.5	48	38.5	17.9
ROI 155	1039	933.3	840	11.3	10.0	487	428.4	348	13.7	18.8	279	223.8	169	24.7	24.5	119	92.5	59	28.6	36.2	69	63.5	58	8.7	8.7
ROI 159	1042	941.7	845	10.7	10.3	493	424.8	313	16.1	26.3	260	226.3	168	14.9	25.8	111	89.8	74	23.6	17.6	78	66.0	52	18.2	21.2
ROI 177	1037	938.1	818	10.5	12.8	468	408.4	313	14.6	23.4	268	213.3	177	25.6	17.0	107	87.7	72	22.0	17.9	79	66.3	58	19.2	12.5
Max NU	17.6%					26.3%					32.7%					36.2%					38.5%				

*Section of the full table that involves 177 regions of interest

concentrations. Accumulation of more counts of activity produces more uniform images and hence, NUs in smaller regions of interest are also lower compared with lesser activity concentrations. Other acquisition parameters such as matrix size and reconstruction algorithms remained constant throughout the study. Average counts of activity per ROI for the 16.87 kBq/mL, 14.06 kBq/mL, 11.25 kBq/mL, 8.43 kBq/mL, and 5.62 kBq/mL activity concentrations were estimated to be 10341.1 cts, 488.3 cts, 280.2 cts, 105.8 cts, and 75.1 cts, respectively.

Coefficients of uniformity variation for the different activity concentrations were estimated to assess the degree of uniformity over the entire surface of the transaxial image slices. The lesser the coefficient of variation, the better the image uniformity and vice versa. The coefficients are estimated in Table 2 and graphically presented in Figure 3. From the results, an inverse quadratic relationship is established with the equation $y = 0.0009x^4 - 0.0320x^3 + 0.3749x^2 - 1.6418x + 7.2007$ at $R^2 = 1$. At constant acquisition factors, increasing activity concentration results in decreasing coefficient of uniformity and hence, an increase in image uniformity. SD estimates, however, showed a linear trend with increasing activity concentration.

Results from the uniformity estimates compare favorably well with NCI's recommendation of an acceptance criterion of less than 10% for axial variation in PET-CT image uniformity.[8] Due to unavailability of reference NU estimates for comparison, acceptance criterion recommended by HHS No. 1[9] could not be assessed. However, with quantitative estimates of uniformity ranging 1.47-4.98% recorded for the different activity concentrations, it could be implied that the acceptance criterion of HHS No. 1 could also be within range. Qualitative assessment of the image slices from different activity concentrations showed relatively better uniformity in the higher activity concentrations than in the lower concentrations.

Conclusion

As part of acceptance testing and quarterly quality control checks of PET-CT systems, PET-CT image uniformity is carried out to assess the system's response to homogeneous activity distribution. This study has quantitatively assessed the level of uniformity in PET-CT image slices that would otherwise have been difficult to accurately predict qualitatively. The study has demonstrated that PET-CT image uniformity is improved with increasing activity concentration at constant acquisition parameters.

Table 2: Coefficient of uniformity variation

ROI	16.87 kBq/mL		14.06 kBq/mL		11.25 kBq/mL		8.43 kBq/mL		5.62 kBq/mL	
	Cts of activity (C_k)	(C_k-Ave** (C_k))^2	Cts of activity (C_k)	(C_k-Ave (C_k))^2	Cts of activity (C_k)	(C_k-Ave (C_k))^2	Cts of activity (C_k)	(C_k-Ave (C_k))^2	Cts of activity (C_k)	(C_k-Ave (C_k))^2
ROI 1	1031	9.6	492	13.7	275	27.0	107	1.6	78	8.4
ROI 2	1023	123.2	495	44.9	292	139.2	100	33.1	73	4.4
ROI 3	1033	1.2	482	39.7	301	432.6	105	0.6	69	37.2
ROI 4	1037	8.4	468	412.1	288	60.8	99	45.7	78	8.4
ROI 5	1036	3.6	495	44.9	261	368.6	100	33.1	75	0.0
ROI 30	1043	79.2	498	94.1	266	201.6	111	27.0	67	65.6
ROI 62	1029	26.0	502	187.7	281	0.6	103	7.8	78	8.4
ROI 151	1022	146.4	503	216.1	289	77.4	99	46.2	81	34.8
ROI 155	1039	24.0	487	1.7	279	1.4	119	175.4	69	37.2
ROI 159	1042	62.4	493	22.1	260	408.0	111	27.0	78	8.4
ROI 177	1037	8.4	468	412.1	268	148.8	107	1.6	79	15.2
Ave	1034.1		488.3		280.2		105.8		75.1	
Σ	183030	40745.4	86423	26632.7	49602	24668.3	18719	5154.6	13285	2459.8
SD	15.22		12.30		11.84		5.41		3.74	
CV	1.47%		2.52%		4.23%		5.12%		4.98%	

*Section of the full table that involves 177 regions of interest. **Ave: Average, CV: Coefficient of variation

References

1. Shreve P, Townsend DW. Clinical PET-CT in Radiology-Integrated Imaging in Oncology. New York, USA: Springer; 2011. p. 26-7, 40-3, 47-8.
2. Kinahan PE, Townsend DW, Beyer T, Sashin D. Attenuation correction for a combined 3D PET/CT scanner. Med Phys 1998;25:2046-53.
3. Kinahan P, Hasegawa B, Beyer T. X-ray-based attenuation correction for positron emission tomography/computed tomography scanners. Semin Nucl Med 2003;33:166-79.
4. Von Schulthess GK. Cost considerations regarding an integrated CT-PET system. Eur Radiol 2000;10(Suppl 3):S377-80.
5. LaCroix KJ, Tsui BMW, Hasegawa BH, Brown JK. Investigation of the use of X-ray CT images for attenuation compensation in SPECT. IEEE Trans Nucl Sci 1994;41:2793-9.
6. Tang HR, Brown JK, Da Silva AJ, Mathay KK, Price DC, Huberty JP, *et al.* Implementation of a combined X-ray CT-scintillation camera imaging system for localizing and measuring radionuclide uptake: Experiments in phantoms and patients. IEEE Trans Nucl Sci 1999;46:551-7.
7. Jadvar H, Parker JA. Clinical PET and PET-CT. New York, USA: Springer; 2005. p. 69-267.
8. Boellaard R, O'Doherty MJ, Weber WA, Mottaghy FM, Lonsdale MN, Stroobants SG, *et al.* FDG PET and PET/CT: EANM procedure guidelines for tumour PET imaging: Version 1.0. Eur J Nucl Med Mol Imaging 2010;37:181-200.
9. American College Radiology Imaging Network. PET-PET/CT Technical Procedures: NCI CQIE Manual of Procedures, Ver 3.2.1: American College Radiology (ACR); 2013. p. 7-9.
10. International Atomic Energy Agency. Quality Assurance for PET and PET-CT Systems: Human Health Series No. 1. Vienna, Austria: International Atomic Energy Agency (IAEA); 2009. p. 125-31.